Non-invasive global-local coupling as a Schwarz domain decomposition method: acceleration and generalization

Pierre Gosselet, Maxime Blanchard, Olivier Allix, Guillaume Guguin

Non-invasive global-local coupling as a Schwarz domain decomposition method: acceleration and generalization

Pierre Gosselet, Maxime Blanchard, Olivier Allix
LMT-Cachan, ENS-Cachan/CNRS/Université Paris Saclay,
61 avenue du Président Wilson, 94235 Cachan, France
gosselet@lmt.ens-cachan.fr, blanchard@ens-cachan.fr,allix@lmt.ens-cachan.fr

October 10, 2017

Abstract

In this paper non-invasive coupling algorithm is revisited and shown to realize a simple implementation of the optimized non-overlapping Schwarz domain decomposition method. This connection is used to propose and compare several acceleration techniques, and to extend the approach to non conforming meshes.

Keywords: non-invasive coupling; Schwarz domain decomposition; non-conforming patch; Krylov acceleration.

1 Introduction

The non-invasive local-global coupling technique proposed by Allix and first implemented in [16] is an iterative technique which aims making accurate the well known submodeling technique [25, 38, 8]. It is strongly related to many reanalysis techniques [24, 42, 43] and domain decomposition methods [22].

The aim of this technique is to evaluate the effect of local modifications inside a computational model (geometry, material and load) without requiring heavy developments. More precisely the objective is to use an industrial model solved on a given commercial software and to simulate the presence of local alterations by iteratively spawning computations with only extra traction loads inside the model. Moreover, the alterations can be computed on any chosen software including dedicated research codes.

This philosophy was successfully applied in many different contexts like: the introduction of local plasticity and geometrical refinements [16], the computation of the propagation of cracks in a sound model [11], the evaluation of stochastic effects with deterministic computations [6], the taking into account of the exact geometry of connectors in an assembly of plates [20]. In [10] the method was used in order to implement a nonlinear domain decomposition method [26, 9, 23, 33] in a non-invasive manner in code_aster. Extension of the approach to explicit dynamics was proposed in [3], improved in [4] and applied to the prediction of delamination under impact loading in [5]. Alternative non-invasive strategies can be derived from the extended finite element method [37, 27].

After a description of the method (section 2), this paper provides several contributions. First the non-invasive coupling algorithm is proved to realize a simple implementation of the optimized non-overlapping Schwarz domain decomposition method (section 3). Then several accelerations techniques are proposed (section 4), some are classical but the linear and nonlinear conjugate gradient is new in this framework. The algorithms are described in a very programmer-friendly manner. Last an overlapping version of the method is proposed (section 5) which can be used to handle fully non-conforming meshes.

2 Derivation of the non-invasive algorithm

The algorithm we study is very general and applies to the study of many PDEs; in order to fix the ideas, we consider problems of nonlinear quasi-static structure mechanics under the small strain hypothesis. We note u the displacement field, ε the symmetric part of the gradient, σ Cauchy's stress tensor. For a domain Ω submitted to given body force f, Dirichlet conditions u_d is imposed on the part $\partial_d\Omega$ of the boundary and Neumann condition g is imposed on the complement part $\partial_n\Omega$. In order to manage viscous materials, the study is conducted over

a time interval $\mathcal{T} = [0, T]$, and the following equations are meant to be satisfied at any time $t \in \mathcal{T}$, which we omit to write except when necessary.

Let $V(\Omega) = \left\{v \in H^1(\Omega), v = u_d \text{ on } \partial_d\Omega\right\}$ be the affine space of admissible displacement and $V^0(\Omega)$ the associated vector space. The conservation of momentum can be written as:

$$\int_\Omega \sigma(u) : \varepsilon(v)\, dx = \int_\Omega f \cdot v\, dx + \int_{\partial_n\Omega} g \cdot v\, dS,\ \forall v \in V^0(\Omega) \tag{1}$$

The notation $\sigma(u)$ stands for local or non linear constitutive laws defined under the following functional expression:

$$\sigma(x,t) = B(\varepsilon(u(x,\tau)), \tau < t),\ x \in \Omega,\ t \in \mathcal{T} \tag{2}$$

This modeling of the mechanical behavior is typically suited for elastoviscoplastic materials. For most models an alternative description by internal variables summarizing the effect of the past history can be found.

The mechanical problem above takes the following classical form:

$$\text{Find } u \in V(\Omega) \ /\ a(u,v) = l(v), \forall v \in V^0(\Omega) \tag{3}$$

where l is a continuous linear form, and a is a continuous coercive form, linear in the second variable, note that a may be nonlinear in the first variable.

In the following we handle several space subdomains and models, when any quantity is specifically attached to one model, a superscript mentions it.

The Reference problem (superscript ^{R}) is set on the domain Ω^R which is the assembly of two non-overlapping subdomains: the zone of interest where a Fine model is required for a reliable simulation (superscript ^{F}), and a Complement zone (superscript ^{C}) where a simpler model is sufficient (and which in general covers most of the structure). The interface is $\Gamma = \partial\Omega^C \cap \partial\Omega^F$, it is thus immersed in Ω^R. Note that using several zones of interest presents no difficulty as long as they do not overlap; note also that the Reference problem is never formed in practice.

$$\textbf{Reference problem} \begin{cases} \text{Find } u \in V(\Omega^R),\ \text{such that } \forall v \in V^0(\Omega^R), \\ a^R(u,v) := a^C(u,v) + a^F(u,v) = l^C(v) + l^F(v) =: l^R(v) \end{cases} \tag{4}$$

We assume that we have another representation of the zone of interest, named Auxiliary representation (superscript ^{A}) which shares the same characteristics as the Complement zone, and which is thus coarser than the Fine representation. Typically if Ω^F was a zone where material coefficients have strong variations, the Fine representation would follow the exact distribution whereas the Auxiliary representation could use a homogeneized behavior; the load could also be simplified. An application is the case where the Fine model is stochastic whereas the Auxiliary model is deterministic [6]. We insert the Auxiliary representation of the zone of interest in the Reference problem:

$$\begin{aligned} &\text{Find } u \in V(\Omega^R), \text{ such that } \forall v \in V^0(\Omega^R), \\ &a^C(u,v) + a^F(u,v) = l^C(v) + l^F(v) \\ &\underbrace{a^C(u,v) + a^A(u,v)}_{a^G(u,v)} = \underbrace{l^C(v) + l^A(v)}_{l^G(v)} + \big(a^A(u,v) - l^A(v)\big) - \big(a^F(u,v) - l^F(v)\big) \end{aligned} \tag{5}$$

The Global problem, (supersript ^{G}), is the assembly of the Complement zone with the Auxiliary (coarse) representation of the zone of interest, this problem is in practice assembled and dealt with by commercial software.

From the previous equation, we could derive the following stationary iteration:

$$a^G(u_{n+1}, v) = l^G(v) + \big(a^A(u_n, v) - l^A(v)\big) - \big(a^F(u_n, v) - l^F(v)\big) \tag{6}$$

which would correspond to a fixed point of the Reference problem preconditioned by the coarse Global system. Not only convergence would be slow but also the right-hand-side terms would not be easy to compute in practice. Moreover, this iteration needs the Auxiliary domain Ω^A to be coincident with the Fine domain Ω^F which is a limitation we want to get rid of. In the following, we only assume that the interface is on the boundary of the Auxiliary domain $\Gamma \subset \partial\Omega^A$, so that Γ is on the boundary of all subdomains. We note V_Γ the trace space of displacements on Γ and V_Γ^* its dual space of interface tractions, $\langle \lambda, v \rangle_\Gamma$ is the associated duality bracket with $\lambda \in V_\Gamma^*$ and $v \in V_\Gamma$.

We thus choose to associate the right hand side of (5) with the evaluation of local problems. Starting from $p_0 = 0$ (the mathematical space for p_n is discussed later), the basic global/local iteration is then the following:

$$\textbf{Global problem} \begin{cases} \text{Find } u_n^G \in V(\Omega^G), \text{ such that } \forall v \in V^0(\Omega^G), \\ a^G(u_n^G, v) = l^G(v) + \langle p_n, v \rangle \end{cases} \tag{7a}$$

$$\textbf{Fine problem} \begin{cases} \text{Find } (u_n^F, \lambda_n^F) \in V(\Omega^F) \times V_\Gamma^*, \text{ s.t. } \forall (v, \mu) \in V^0(\Omega^F) \times V_\Gamma^*, \\ \begin{cases} a^F(u_n^F, v) = l^F(v) + \langle \lambda_n^F, v \rangle_\Gamma \\ \langle \mu, u_n^F - u_n^G \rangle_\Gamma = 0 \end{cases} \end{cases} \tag{7b}$$

$$\textbf{Auxiliary problem} \begin{cases} \text{Find } (u_n^A, \lambda_n^A) \in V(\Omega^A) \times V_\Gamma^*, \text{ s.t. } \forall (v, \mu) \in V^0(\Omega^A) \times V_\Gamma^*, \\ \begin{cases} a^A(u_n^A, v) = l^A(v) + \langle \lambda_n^A, v \rangle_\Gamma \\ \langle \mu, u_n^A - u_n^G \rangle_\Gamma = 0 \end{cases} \end{cases} \tag{7c}$$

$$\textbf{Update} \begin{cases} \langle p_{n+1}, v \rangle = \left(a^A(u_n^A, v^A) - l^A(v^A)\right) - \left(a^F(u_n^F, v^F) - l^F(v^F)\right) \\ \text{with } v_{|\Gamma}^A = v_{|\Gamma}^F = v \end{cases} \tag{7d}$$

In words, the Global problem is the coarse problem with extra load p, the Fine and Auxiliary systems are resolutions on the domain of interest with imposed Dirichlet conditions on Γ. We chose a Lagrangian formulation for these problems in order to make appear the reaction forces λ^F and λ^A. The update is simply the equivalent of (6) with fields issuing from the local solves instead of the global one.

Remark 1. Of course, the Lagrange multipliers are equal to the normal stress:

$$\lambda^X = \sigma^X \cdot n^X \tag{8}$$

where $X \in \{A, F\}$ and n^X is the outer normal vector. □

We have the following properties:

- Assuming the fine and auxiliary problems were solved exactly, we have:

$$p_{n+1} = \left(\lambda_n^A - \lambda_n^F\right) \in V_\Gamma^* \tag{9}$$

  the corrective load p is then an immersed surface traction. In the following, we always assume the exactness of the resolution; note that using inexact solvers was investigated in [35] where the method is identified with a localized multigrid iteration.

- Because the Auxiliary problem corresponds to the restriction of the Global problem on the zone of interest with global displacement imposed, we directly have:

$$u_n^A = u_{n|\Omega^A}^G \tag{10}$$

  The introduction of the Auxiliary problem is thus not mandatory, it is just a workaround in case of software unable to compute the reaction in an immersed surface. Of course, the Auxiliary problem can be solved in parallel with the Fine problem.

- We can also define the reaction from the Complement zone:

$$a^C(u_n^G, v) = l^C(v) + \langle \lambda_n^C, v \rangle_\Gamma, \ \forall v \in V(\Omega^C) \tag{11}$$

  Then we see that:

$$\lambda_n^C + \lambda_n^A = p_n \tag{12}$$

  The surface traction p_n generates a discontinuity in the normal stress of the Global problem.

- If we replace the auxiliary reaction by the complement one, we have:

$$p_{n+1} = p_n + r_n \text{ with } r_{n+1} = -\left(\lambda_n^F + \lambda_n^C\right) \tag{13}$$

  in words, the correction brought to p_{n+1} corresponds to the lack of balance between the Complement zone and the Fine representation of the zone of interest. This lack of balance is the residual r of the algorithm. The algorithm converges when the two representations are in equilibrium ($r = 0$, in which case the extra load p shall not evolve anymore).

- The algorithm makes no use of domain integrals to communicate between subdomains; only interface data (on Γ) are exchanged, namely the displacement u^G and the reactions λ^F and λ^A (or λ^C). As long as the interface Γ is well represented in all models, it is not necessary to use the exact Fine domain Ω^F in the Auxiliary problem, any coarser representation is possible (Ω^A). Typically micro-perforations or micro cracks need not be represented in the Auxiliary problem. Of course modifying the representation of the zone of interest may have consequences on the convergence of the algorithm (but not on its limit which is the reference solution).

3 Connexion with alternate non-overlapping Schwarz method

The question of linking the non-invasive global-local coupling method to the many variants of domain decomposition and associated algorithms, like *chimera*, was studied in other publications like [22]. Here we propose to connect the method with the iterations of a non-overlapping optimized Schwarz method. The theoretical framework of Schwarz method will allow us natural extensions to the method, in particular the use of overlaps to treat mesh incompatibilities.

We consider two non-overlapping subdomains, Ω^C and Ω^F, connected by Interface Γ. The decomposed problem to solve can be written as:

$$\textbf{Fine equilibrium} \begin{cases} (u^F, \lambda^F) \in V(\Omega^F) \times V_\Gamma^*, \text{ s.t. } \forall v \in V^0(\Omega^F), \\ a^F(u^F, v) = l^F(v) + \langle \lambda^F, v \rangle_\Gamma \end{cases} \tag{14a}$$

$$\textbf{Complement equilibrium} \begin{cases} (u^C, \lambda^C) \in V(\Omega^C) \times V_\Gamma^*, \text{ s.t. } \forall v \in V^0(\Omega^C), \\ a^C(u^C, v) = l^C(v) + \langle \lambda^C, v \rangle_\Gamma \end{cases} \tag{14b}$$

$$\textbf{Interface conditions} \begin{cases} \langle \lambda_F + \lambda_C, v \rangle_\Gamma = 0, \ \forall v \in V_\Gamma \\ \langle \mu, u^F - u^C \rangle_\Gamma = 0, \ \forall \mu \in V_\Gamma^* \end{cases} \tag{14c}$$

In words subdomains must be in mechanical equilibrium while displacements shall be equal on the interface and force fluxes shall be balanced. The optimized Schwarz method consists in using Robin conditions at the interface. The Robin conditions are materialized by operators called interface impedances (or interface stiffnesses): Q^C and Q^F from V_Γ to V_Γ^*.The interface conditions are rewritten as:

$$\begin{aligned} (\lambda^F + \lambda^C) - Q^C(u^F) + Q^C(u^C) = 0 \\ (\lambda^F + \lambda^C) + Q^F(u^F) - Q^F(u^C) = 0 \end{aligned} \tag{15}$$

where we need in particular $(Q^C + Q^F)$ to be injective for the equivalence with initial conditions to hold. In general Q^C and Q^F are chosen to be such that each associated form $V_\Gamma^2 \ni (u, v) \mapsto \langle Q^X(u), v \rangle_\Gamma$ is bilinear symmetric continuous coercive.

The new conditions can be combined with the equilibrium:

$$\begin{aligned} a^F(u^F, v) + \langle Q^F(u^F), v \rangle_\Gamma = l^F(v) + \langle Q^F(u^C) - \lambda^C, v \rangle_\Gamma, \ \forall v \in V(\Omega^F) \\ a^C(u^C, v) + \langle Q^C(u^C), v \rangle_\Gamma = l^C(v) + \langle Q^C(u^F) - \lambda^F, v \rangle_\Gamma, \ \forall v \in V(\Omega^C) \end{aligned} \tag{16}$$

Hence the alternate optimized Schwarz stationary iterations ($\lambda_0^F = 0$, $u_0^F = 0$):

$$\begin{aligned} &\textbf{Find } u^C_{n+\frac{1}{2}} \in V(\Omega^C) \text{ s.t. } \forall v \in V(\Omega^C), \\ &\qquad a^C(u^C_{n+\frac{1}{2}}, v) + \langle Q^C(u^C_{n+\frac{1}{2}}), v \rangle_\Gamma = l^C(v) + \langle Q^C(u^F_n) - \lambda^F_n, v \rangle_\Gamma \\ &\textbf{Compute } \lambda^C_{n+\frac{1}{2}} \in V_\Gamma^* \text{ s.t. } \forall v \in V_\Gamma, \ a^C(u^C_{n+\frac{1}{2}}, v) = l^C(v) + \langle \lambda^C_{n+\frac{1}{2}}, v \rangle_\Gamma \\ &\textbf{Find } u^F_{n+1} \in V(\Omega^F) \text{ s.t. } \forall v \in V(\Omega^F), \\ &\qquad a^F(u^F_{n+1}, v) + \langle Q^F(u^F_{n+1}), v \rangle_\Gamma = l^C(v) + \langle Q^F(u^C_{n+\frac{1}{2}}) - \lambda^C_{n+\frac{1}{2}}, v \rangle_\Gamma \\ &\textbf{Compute } \lambda^F_{n+1} \in V_\Gamma^* \text{ s.t. } \forall v \in V_\Gamma, \ a^F(u^F_{n+1}, v) = l^F(v) + \langle \lambda^F_{n+1}, v \rangle_\Gamma \end{aligned} \tag{17}$$

It is well known that the optimal value for one subdomain's impedance is the Dirichlet-to-Neumann operator

of the other subdomain which we note $\mathcal{S}^X$. Typically for Ω^C, we have:

$$\begin{aligned} &Q^C_{opt} = \mathcal{S}^F :\ V_\Gamma \ni u_\Gamma \mapsto \mathcal{S}^F(u_\Gamma) = \lambda^F \in V_\Gamma^*,\ \text{where} \\ &(u^F, \lambda^F) \in V(\Omega^F) \times V_\Gamma^* \text{ are such that } \forall (v,\mu) \in V^0(\Omega^F) \times V_\Gamma^*, \\ &a^F(u^F, v) = l^F(v) + \langle \lambda^F, v\rangle_\Gamma \text{ and } \langle \mu, u^F - u_\Gamma\rangle_\Gamma = 0 \end{aligned} \tag{18}$$

Note that in for linear problems, $\mathcal{S}^X$ is an affine operator (and not just a linear operator) since it also takes into account the effect of the load. The existence of this operator is conditioned to the well-posedness of the Dirichlet problem over subdomains. There are many contexts where this well-posedness can be proved, at least locally, see for instance [7] for details. The global existence of the operator can be proved in the case of coercive continuous monotone operators; see for instance [40, 41] for an analysis at the level of the variational formulation and [12] for the analysis of the finite element approximation. Mechanically this case is associated with positive hardening behaviors and certain contact laws, in small strains [28, 29]. Moreover, the Dirichlet-to-Neumann operator inherits properties from the initial problem (typically monotonicity, coercivity and continuity; see for instance [21] and associated bibliography).

The global-local algorithm corresponds to the choice $Q^C = \mathcal{S}^A$ and formally $Q^F = \infty$ (the Dirichlet condition being seem as the limit case of an infinite interface impedance). The choice $Q^C = \mathcal{S}^A$ is extremely strong because the can expect $\mathcal{S}^A$ to be a good approximation of $\mathcal{S}^F$; not only in term of stiffness (a^A vs a^F) but also in term of load (l^A vs l^F) which corresponds to providing a good initialization to the algorithm.

The framework of Schwarz method enables us to recover the following features:

- Krylov acceleration: replacing stationary iterations by Krylov solvers is classical in Schwarz methods [14]. The Dirichlet condition $Q^F = \infty$ preserves some symmetry so that we can derive a conjugate gradient algorithm, see section 4.4.
- Mixed approach: the condition $Q^F = \infty$ is a poor approximation of the optimal choice. Many work exist on how to improve this approximation [13]. In [15] a two scale approximation of $\mathcal{S}^C$ was proposed.
- Parallel processing: the global-local method corresponds to the multiplicative version of the optimized Schwarz method. The additive (parallel) version could be tried in the non-invasive context. Note that this would only make sense in the presence of multiple Fine zones with finite Fine impedance $Q^F < \infty$.
- Nonlinearity: stationary iterations can directly be transferred to nonlinear problems, in particular the ones with monotone operators (positive hardening) [1, 30]. The local-global method was successfully applied in many nonlinear problems like plasticity or cracking [16, 35]
- Overlapping version: optimized Schwarz methods also exist with overlaps. In [19], the overlap was used as a buffer zone to dampen edge effects in plate/3D coupling. In section 5, we present another application, the handling of non-matching meshes.

4 Analysis and acceleration of the global/local algorithm

4.1 Notations

In order to further analyze the algorithm and be more practical, we now consider the finite element discretization of the problem. We use the following notations: $\mathbf{f}$ for the generalized forces, $\mathbf{u}$ for the nodal displacement and $\boldsymbol{\lambda}$ for the nodal reactions and $\mathbf{p}$ for the nodal component on the immersed surface effort. When indexing degrees of freedom, F, A, C stand for the internal degrees of freedom whereas Γ stands for nodes on the interface (whose description is identical in all models). We tried to use minimal notations, but sometimes a quantity defined on the interface is issued from one side specifically, in which case we make it clear by an extra superscript. In the linear(ized) case notation $\mathbf{K}$ is used for the stiffness matrices.

Remark 2. We recall that the nodal reaction is not the discretization of the Lagrange multiplier. Indeed for a boundary degree of freedom i associated with shape function ϕ_i, we have:

$$\begin{aligned} \boldsymbol{\lambda}^X_i &= \int_{\Omega^X} (\sigma_h : \varepsilon(\phi_i) - f\cdot\phi_i)\, dx - \int_{\partial_n\Omega^X} g\cdot\phi_i\, dS \\ &= \int_\Gamma (\sigma^X_h \cdot n^X)\cdot\phi_i\, dS - \int_{\Omega^X} (\operatorname{div}(\sigma_h) + f)\cdot\phi_i\, dx + \int_{\partial_n\Omega} \big(\sigma_h\cdot n^X - g\big)\cdot\phi_i\, dS \end{aligned} \tag{19}$$

where $X \in \{C, A, F\}$, n^X is the outer normal vector and σ_h is the stress tensor obtained from the finite element computation. Thus the nodal reactions $\boldsymbol{\lambda}^X$ can be computed either by using a Lagrangian formulation for the Dirichlet condition (which is fairly common in commercial software) or by using the formula above to post-process it from the finite element stress (which may be complex to implement in legacy software); hence the use of the Auxiliary model to compute reactions on the immersed interface. □

If we assume that the Reference and the Global problems are well-posed, then Dirichlet problems are well posed on all subdomains, at least locally near the solution. We can then define the following nonlinear discrete Dirichlet-to-Neumann operators $\mathcal{S}^X$ (we use the same notation as in the continuous case) which compute the reactions $\boldsymbol{\lambda}^X$ from a given interface displacement $\mathbf{u}_\Gamma$:

$$\begin{aligned} \text{Fine problem (7b)} &: \boldsymbol{\lambda}^F = \mathcal{S}^F(\mathbf{u}_\Gamma; \mathbf{f}^F) \\ \text{Auxiliary problem (7c)} &: \boldsymbol{\lambda}^A = \mathcal{S}^A(\mathbf{u}_\Gamma; \mathbf{f}^A) \\ \text{Complement problem} &: \boldsymbol{\lambda}^C = \mathcal{S}^C(\mathbf{u}_\Gamma; \mathbf{f}^C) \end{aligned} \tag{20}$$

Because of the nonlinearity, the effects of given loads appear as parameter of the method, they will be omitted in the absence of ambiguity.

Remark 3. In the case of linear problems, it is possible to give an explicit formula for the Dirichlet-to-Neumann operators. As an illustration, the equilibrium of the Fine problem writes:

$$\begin{pmatrix} \mathbf{K}^F_{\Gamma\Gamma} & \mathbf{K}_{\Gamma F} \\ \mathbf{K}_{F\Gamma} & \mathbf{K}_{FF} \end{pmatrix} \begin{pmatrix} \mathbf{u}_\Gamma \\ \mathbf{u}^F \end{pmatrix} = \begin{pmatrix} \mathbf{f}^F_\Gamma \\ \mathbf{f}^F \end{pmatrix} + \begin{pmatrix} \boldsymbol{\lambda}^F \\ 0 \end{pmatrix} \tag{21}$$

which can be condensed as:

$$\boldsymbol{\lambda}^F = \mathcal{S}^F(\mathbf{u}, \mathbf{f}^F) = \mathbf{S}^F \mathbf{u}_\Gamma - \mathbf{b}^F \text{ with } \begin{cases} \mathbf{S}^F = \mathbf{K}^F_{\Gamma\Gamma} - \mathbf{K}_{\Gamma F}\mathbf{K}^{-1}_{FF}\mathbf{K}_{F\Gamma} \\ \mathbf{b}^F = \mathbf{f}^F_\Gamma - \mathbf{K}_{\Gamma F}\mathbf{K}^{-1}_{FF}\mathbf{f}^F \end{cases} \tag{22}$$

In that case, $\mathcal{S}^F$ is an affine operator: $\mathbf{S}^F$ is the well known Schur complement of the Fine domain on the interface. Linearity allows to set apart the contrition of the given load, with $\mathbf{b}^F$ the condensed right-hand side. Note that the internal displacement in the Fine domain was implicitly computed as:

$$\mathbf{u}^F = \mathbf{K}^{-1}_{FF}\left(\mathbf{f}^F - \mathbf{K}_{F\Gamma}\mathbf{u}_\Gamma\right) \tag{23}$$

□

Because of the additivity of integral with respect to the domain, the Global operator verifies the following decomposition $\mathcal{S}^G = \mathcal{S}^C + \mathcal{S}^A$ and the Reference operator writes $\mathcal{S}^R = \mathcal{S}^C + \mathcal{S}^F$, and we can rephrase the Global and Reference problems in a condensed manner:

$$\begin{aligned} \text{Reference problem (4), } \mathbf{u}_\Gamma ?\ \mathcal{S}^R(\mathbf{u}_\Gamma; \mathbf{f}^R) = \mathcal{S}^C(\mathbf{u}_\Gamma; \mathbf{f}^C) + \mathcal{S}^F(\mathbf{u}_\Gamma; \mathbf{f}^F) = 0 \\ \text{Global problem (7a), } \mathbf{u}_\Gamma ?\ \mathcal{S}^G(\mathbf{u}_\Gamma; \mathbf{f}^G) = \mathcal{S}^C(\mathbf{u}_\Gamma; \mathbf{f}^C) + \mathcal{S}^A(\mathbf{u}_\Gamma; \mathbf{f}^A) = \mathbf{p} \end{aligned} \tag{24}$$

Note that each time one of the condensed operators is employed, the displacement inside the subdomains is implicitly computed: for instance, $\mathbf{u}^G$ in a by-product of (24) and $\mathbf{u}^F$ in a by-product of (20). To make it clearer, we will use notations $\mathcal{S}^X$ when analyzing the methods, whereas we will use the following functional notations when describing the algorithms:

- $[\mathbf{u}^G] = \texttt{SolveGlobal}(\mathbf{p}; \mathbf{f}^G)$, $\mathbf{u}^G$ is defined on the whole Global model and in particular we have $\mathbf{u}^G_\Gamma = \mathcal{S}^{G^{-1}}(\mathbf{p}; \mathbf{f}^G)$.
- $[\mathbf{u}^F, \boldsymbol{\lambda}^F] = \texttt{SolveFine}(\mathbf{u}^G; \mathbf{f}^F)$, $\mathbf{u}^F$ is defined in the Fine model and we have $\boldsymbol{\lambda}^F = \mathcal{S}^F(\mathbf{u}^G_\Gamma; \mathbf{f}^F)$
- $[\boldsymbol{\lambda}^A] = \texttt{SolveAux}(\mathbf{u}^G; \mathbf{f}^A)$, which in corresponds to $\boldsymbol{\lambda}^A = \mathcal{S}^A(\mathbf{u}^G_\Gamma; \mathbf{f}^A)$. When authorized by the software, it can be replaced by the post-processing of the stress (19).

The Fine and Auxiliary solves are in general gathered in one line because the computations can be run in parallel.

In order to keep notations simple, we assume the coarse and fine meshes are conforming at the interface. In most cases the zone of interest is deduced from an initial coarse computation and it is defined as a subset of

coarse elements. Then the interface Γ lies on faces of coarse elements and it defines the boundary of the Fine domain. In that context, even if the Fine discretization is chosen to be finer than the Global one on Γ, a simple Global-master – Fine-slave strategy may give satisfying results: a transfer matrix $\mathbf{T}$ is computed (for instance using interpolation or Mortar techniques) such that the interface conditions can be written as:

$$\mathbf{T}\mathbf{u}_\Gamma^C - \mathbf{u}_\Gamma^F = 0 \qquad \text{and} \qquad \boldsymbol{\lambda}^C + \mathbf{T}^T\boldsymbol{\lambda}^F = 0 \tag{25}$$

so that the mechanical work is preserved. The algorithms presented below are unchanged, one just need to consider the Global interface as the master interface. Note that Section 5 presents a technique to handle non-coincident interfaces.

4.2 Stationary iterations

The global/local coupling iterations of equation (7) can formally be written as:

$$\begin{aligned}\mathbf{p}_{n+1} &= (\mathcal{S}^A - \mathcal{S}^F) \circ \mathcal{S}^{G^{-1}}(\mathbf{p}_n) \\ &= \mathbf{p}_n - \mathcal{S}^R \circ \mathcal{S}^{G^{-1}}(\mathbf{p}_n)\end{aligned} \tag{26}$$

One recognizes fixed point iterations. The convergence is controlled by the contraction property of the operator $I - \mathcal{S}^R \circ \mathcal{S}^{G^{-1}} = (\mathcal{S}^A - \mathcal{S}^F) \circ (\mathcal{S}^A + \mathcal{S}^C)^{-1}$.

Remark 4. In the linear case, the operator that controls the convergence can be written as:

$$(\mathbf{S}^A - \mathbf{S}^F)(\mathbf{S}^A + \mathbf{S}^C)^{-1} \tag{27}$$

since all Schur complements are symmetric positive definite, a trivial sufficient condition for the operator to be a contraction is $\mathbf{S}^A \geqslant \mathbf{S}^F$ (for the quadratic norm ordering). Mechanically speaking this means that the Auxiliary model shall be stiffer that the Fine one; this is usually the case when the Fine model has a refined mesh or holes. Moreover, we can expect the Auxiliary model to be a good approximation of the Fine model leading to ($\mathbf{S}^A \simeq \mathbf{S}^F$) and fast convergence. □

A classical tweak for fixed point iterations is to use relaxation. This enables to grant contraction property or to improve the convergence rate. In that case, the iteration writes:

$$\mathbf{p}_{n+1} = \mathbf{p}_n - \omega_n \, \mathcal{S}^R \circ \mathcal{S}^{G^{-1}}(\mathbf{p}_n), \qquad |\omega| > \epsilon > 0 \tag{28}$$

For linear problems, it is well known that convergence is ensured for $0 < \omega < 2/\rho\left(\mathbf{S}^{G^{-1}}\mathbf{S}^R\right)$ and the optimal value is $\omega = 2/(\lambda_{\min} + \lambda_{\max})$ where the λs' stand for the minimal and maximal eigenvalues of $\mathbf{S}^{G^{-1}}\mathbf{S}^R$. An alternative, when the area to be reanalyzed is known a priori, would be to choose the global model in order for the auxiliary model to be slightly stiffer than the local one.

The results of the existence of sufficient and of optimal relaxations can be extended to the case of a monotone problem. Indeed in that case, the method can be interpreted as an operator splitting technique [39] on the condensed problem which inherits the useful properties of the original system (in particular monotonicity and coercivity). Reader may refer to [34] for detailed proof with weak assumptions.

In practice, it is convenient to have ω adapted at each step. A good heuristic for the sequence (ω_n) is provided by Aitken's Δ^2. It was first tried in the global/local framework in [31]. The strategy is summed-up in algorithm 1.

4.3 Quasi-Newton's approaches for linear Global model

The system to solve associated to the fixed point iterations (26) writes:

$$\text{Find } \mathbf{p} \;/\; \mathcal{S}^R \circ \mathcal{S}^{G^{-1}}(\mathbf{p}) = 0 \tag{29}$$

which mechanically means that we seek the surface traction to impose inside the Global coarse model (ie the stress discontinuity) such that the Fine model with Dirichlet conditions issued from the Global solve is in balance with the Complement zone.

Algorithm 1: Non-invasive stationary iterations with relaxation

Arbitrary initialization $\mathbf{p}_0$
for $j \in [0, \cdots, m]$ **do**
  $[\mathbf{u}_j^G] = \texttt{SolveGlobal}(\mathbf{p}_j; \mathbf{f}^G)$
  $[\mathbf{u}_j^F, \boldsymbol{\lambda}_j^F] = \texttt{SolveFine}(\mathbf{u}_j^G; \mathbf{f}^F)$ // $[\boldsymbol{\lambda}_j^A] = \texttt{SolveAux}(\mathbf{u}_j^G; \mathbf{f}^A)$
  Residual: $\mathbf{r}_j = -(\boldsymbol{\lambda}_j^F + \mathbf{p}_j - \boldsymbol{\lambda}_j^A)$
  Update: $\mathbf{p}_{j+1} = \mathbf{p}_j + \mathbf{r}_j$;
  Aitken Δ^2: $\mathbf{p}_{j+1} \leftarrow \omega_{j+1}\mathbf{p}_{j+1} + (1-\omega_{j+1})\mathbf{p}_j$ with $\omega_{j+1} = -\omega_j \frac{\mathbf{r}_{j-1}^T(\mathbf{r}_j - \mathbf{r}_{j-1})}{\|\mathbf{r}_j - \mathbf{r}_{j-1}\|^2}$
end

Applying a Newton iteration to system (29) leads to the sequence:

$$\left(\mathbf{D}\mathcal{S}^R\right)\left(\mathbf{D}\mathcal{S}^G\right)^{-1}(\mathbf{p}_{n+1} - \mathbf{p}_n) = -\mathcal{S}^R \circ \mathcal{S}^{G^{-1}}(\mathbf{p}_n) \tag{30}$$

which was investigated in nonlinear relocalization techniques [33, 9, 36, 23]. but which is is not possible in general in a non-invasive framework. Anyhow, in the case of a linear Global model, it is possible to derive a quasi-Newton approach.

If the Global problem is linear then the differential of the Global problem is constant and it is equal to the Schur complement $\mathbf{D}\mathcal{S}^G = \mathbf{S}^G$. Regarding the nonlinear part, we have:

$$\mathbf{D}\mathcal{S}^R = \mathbf{S}^C + \mathbf{D}\mathcal{S}^F = \underbrace{\mathbf{S}^C + \mathbf{S}^A}_{\mathbf{S}^G} + \underbrace{\mathbf{D}\mathcal{S}^F - \mathbf{S}^A}_{\mathbf{X}} \tag{31}$$

of course $\mathbf{X}$ is not computable in a non-invasive manner, but a low rank approximation is possible using quasi-Newton formulas. In particular, SR1 formula was tried with success in [16]. In practice, line search is not applied which makes the low rank update slightly lighter than usual, we note $\boldsymbol{\delta}_j^u = (\mathbf{u}_j - \mathbf{u}_{j-1})_{|\Gamma}$ and $\boldsymbol{\delta}_j^p = (\mathbf{p}_j - \mathbf{p}_{j-1})$, the increment of the interface quantities:

$$\begin{aligned}
\mathbf{D}\mathcal{S}_{R,0} &= \mathbf{S}^G \\
\mathbf{D}\mathcal{S}_{R,i} &= \mathbf{D}\mathcal{S}_{R,i-1} + \frac{\mathbf{r}_{i-1}\mathbf{r}_{i-1}^T}{\mathbf{r}_{i-1}^T\boldsymbol{\delta}_{i-1}^u} \\
&= \mathbf{S}^G + \mathbf{R}_i\boldsymbol{\Delta}_i^{-1}\mathbf{R}_i^T
\end{aligned} \tag{32}$$

with, for $i > 0$, $\mathbf{R}_i = [\mathbf{r}_1 \dots \mathbf{r}_i]$ and $\boldsymbol{\Delta}_i = \mathrm{diag}(\mathbf{r}_i^T\boldsymbol{\delta}_i^u)$. Sherman-Morrison formula leads to:

$$\mathbf{D}\mathcal{S}_{R,i}^{-1} = \mathbf{S}^{G^{-1}} - \mathbf{S}^{G^{-1}}\mathbf{R}_i\left(\boldsymbol{\Delta}_i + \mathbf{R}_i^T\mathbf{S}^{G^{-1}}\mathbf{R}_i\right)^{-1}\mathbf{R}_i^T\mathbf{S}^{G^{-1}} \tag{33}$$

It makes sense to first evaluate $\mathbf{S}^{G^{-1}}\mathbf{r}_i$ then apply corrections. For efficiency reasons, we also store the matrix $\mathbf{W}_i := \mathbf{S}^{G^{-1}}\mathbf{R}_i$. The factorization of Matrix $\left(\boldsymbol{\Delta}_i + \mathbf{R}_i^T\mathbf{S}^{G^{-1}}\mathbf{R}_i\right)$ is reused from one iteration to another, only one row and column must be computed. The method is recapitulated in the algorithm 2. Note that this algorithm is written in a way which makes no use of the linearity of the Global problem, so that it will be also tested in the full nonlinear case.

4.4 Conjugate gradient

4.4.1 Full linear case

This case occurs when all models are linear. Non-invasive global/local coupling can still be of interest in order to introduce complex local heterogeneities, stochastic behaviors or complex geometries in the Fine model.

For linear problems, it is rather classical to use Krylov accelerator on a stationary iteration. In our case, the problem to solve (29) is governed by the operator $\mathbf{S}^R\mathbf{S}^{G^{-1}}$ which is symmetric in the $\mathbf{S}^{G^{-1}}$ inner-product. We then can derive a right-preconditioned conjugate gradient. The algorithm being not so standard, it is given in algorithm 3.

Beside the improved convergence compared to stationary iterations, using conjugate gradient allows an unconditional convergence (without necessity for the Auxiliary model to be stiffer than the Fine model).

Algorithm 2: Non-invasive SR1 Quasi-Newton iterations

Arbitrary initialization $\mathbf{p}_0$
$[\mathbf{u}_0^G] = \texttt{SolveGlobal}(\mathbf{p}_0; \mathbf{f}^G)$
$[\mathbf{u}_0^F, \boldsymbol{\lambda}_0^F] = \texttt{SolveFine}(\mathbf{u}_0^G; \mathbf{f}^F)$ // $[\boldsymbol{\lambda}_0^A] = \texttt{SolveAux}(\mathbf{u}_0^G; \mathbf{f}^A)$
Residual: $\mathbf{r}_0 = -(\boldsymbol{\lambda}_0^F + \mathbf{p}_0 - \boldsymbol{\lambda}_0^A)$
Set $\mathbf{W}_0 = []$, $\mathbf{R}_0 = []$, $\mathbf{x}_1 = 0$
for $j \in [1, \cdots, m]$ **do**
  $\mathbf{p}_j = \boldsymbol{\lambda}_{j-1}^A - \boldsymbol{\lambda}_{j-1}^F$
  $[\tilde{\mathbf{u}}_j^G] = \texttt{SolveGlobal}(\mathbf{p}_j; \mathbf{f}^G)$
  if $j > 1$ **then**
    Set: $\mathbf{W}_{j-1} = [\mathbf{W}_{j-2}, \tilde{\mathbf{u}}_j^G - \mathbf{u}_j^G]$
    Compute: $\mathbf{x}_j = (\boldsymbol{\Delta}_{j-1} + \mathbf{W}_{j-1}^T \mathbf{R}_{j-1})^{-1} \mathbf{W}_{j-1}^T \mathbf{r}_{j-1}$
  end
  Corrector $\mathbf{u}_j^G = \tilde{\mathbf{u}}_j^G - \mathbf{W}_j \mathbf{x}_j$
  Set: $\boldsymbol{\delta}_j^u = \mathbf{u}_{j|\Gamma} - \mathbf{u}_{j-1|\Gamma}$, $\boldsymbol{\Delta}_j = \mathrm{diag}(\boldsymbol{\delta}_i^u)_{1 \leqslant i \leqslant j}$
  $[\mathbf{u}_j^F, \boldsymbol{\lambda}_j^F] = \texttt{SolveFine}(\mathbf{u}_j^G; \mathbf{f}^F)$ // $[\boldsymbol{\lambda}_j^A] = \texttt{SolveAux}(\mathbf{u}_j^G; \mathbf{f}^A)$
  Residual: $\mathbf{r}_j = -(\boldsymbol{\lambda}_j^F + \mathbf{p}_j - \boldsymbol{\lambda}_j^A)$, $\mathbf{R}_j = [\mathbf{R}_{j-1}, \mathbf{r}_j]$
end

Algorithm 3: Non-invasive right-preconditioned conjugate gradient

Arbitrary initialization $\mathbf{p}_0 = \mathbf{0}$
$[\mathbf{u}_0^G] = \texttt{SolveGlobal}(\mathbf{p}_0; \mathbf{f}^G)$
$[\mathbf{u}_0^F, \boldsymbol{\lambda}_0^F] = \texttt{SolveFine}(\mathbf{u}_0^G; \mathbf{f}^F)$ // $[\boldsymbol{\lambda}_0^A] = \texttt{SolveAux}(\mathbf{u}_0^G; \mathbf{f}^A)$
Post-process:
$\boldsymbol{\lambda}_0^C = \mathbf{p}_0 - \boldsymbol{\lambda}_0^A$
$\mathbf{r}_0 = -(\boldsymbol{\lambda}_0^F + \boldsymbol{\lambda}_0^C)$
Initialization: $\underline{\mathbf{p}}_0 = \mathbf{r}_0$
Preconditioning: $[\underline{\mathbf{u}}_0^G] = \texttt{SolveGlobal}(\mathbf{p}_0 + \mathbf{r}_0; \mathbf{f}^G) - [\mathbf{u}_0^G]$
$\mathbf{y} = \underline{\mathbf{u}}_0^G$
for $j \in [0, \cdots, m]$ **do**
  $[\underline{\mathbf{u}}_j^F, \underline{\boldsymbol{\lambda}}_j^F] = \texttt{SolveFine}(\mathbf{y} + \mathbf{u}_j^G; \mathbf{f}^A) - [\mathbf{u}_j^F, \boldsymbol{\lambda}_j^F]$ // $\quad \cdots \; [\underline{\boldsymbol{\lambda}}_j^A] = \texttt{SolveAux}(\mathbf{y} + \mathbf{u}_j^G; \mathbf{f}^A) - [\boldsymbol{\lambda}_j^A]$
  Post-process: $d\boldsymbol{\lambda}_j^C = \mathbf{p}_j + \underline{\mathbf{p}}_j - [\boldsymbol{\lambda}_j^A + \underline{\boldsymbol{\lambda}}_j^A] - \boldsymbol{\lambda}_j^C$
  Direction of the variation of the residual: $\underline{\mathbf{r}}_j = \underline{\boldsymbol{\lambda}}_j^F + \underline{\boldsymbol{\lambda}}_j^C$
  Optimal step size: $\alpha_j = (\mathbf{r}_j^T \mathbf{y})/(\mathbf{y}^T \underline{\mathbf{r}}_j)$
  Updates: $\mathbf{p}_{j+1} = \mathbf{p}_j + \alpha_j \underline{\mathbf{p}}_j$; $\mathbf{r}_{j+1} = \mathbf{r}_j - \alpha_j \underline{\mathbf{r}}_j$
  $\mathbf{u}_{j+1}^G = \mathbf{u}_j^G + \alpha_j \mathbf{y}$; $\mathbf{u}_{j+1}^F = \mathbf{u}_j^F + \alpha_j \underline{\mathbf{u}}_j^F$; $\boldsymbol{\lambda}_{j+1}^{C,A,F} = \boldsymbol{\lambda}_j^{C,A,F} + \alpha_j \underline{\boldsymbol{\lambda}}_j^{C,A,F}$
  Preconditioning: $[\underline{\tilde{\mathbf{u}}}_{j+1}^G] = \texttt{SolveGlobal}(\mathbf{p}_{j+1} + \mathbf{r}_{j+1}; \mathbf{f}^G) - [\mathbf{u}_{j+1}^G]$
  Orthogonalization: $\underline{\mathbf{p}}_{j+1} = \mathbf{r}_{j+1} - \beta_j \underline{\mathbf{p}}_j$ with $\beta_j = -(\underline{\mathbf{r}}_j^T \underline{\tilde{\mathbf{u}}}_{j+1})/(\underline{\mathbf{r}}_j^T \mathbf{y})$
  Correction: $\mathbf{y} = \underline{\tilde{\mathbf{u}}}_{j+1}^G + \beta_j \mathbf{y}$
end

4.4.2 Nonlinear case

Conjugate gradient can be extended to nonlinear cases using two ingredients:

- A line search algorithm to optimize the length of the steps. For a given search direction $\underline{\mathbf{p}}$, one tries to find the optimal length α in term of the minimization of some norm of the residual. This can be done in a non-invasive manner by a sampling technique with several lengths (α_i) being tested in parallel. Classically these samples are used to interpolate the objective function and decide the final α. Because of the cost of the estimation of one configuration (one global solve followed by one local solve), we prefer to use directly the best sample already computed (except if the interpolated minimal let us expect a significantly better configuration).

- A "conjugation" technique for the new search direction $\underline{\mathbf{p}}_{j+1} = -\mathbf{r}_{j+1} + \beta_j \underline{\mathbf{p}}_j$ given by a heuristic (using the notations of algorithm 4) like:

$$\begin{aligned} &\text{Fletcher-Reeves: } \beta_j = \frac{\mathbf{r}_{j+1}^T \mathbf{r}_{j+1}}{\mathbf{r}_j^T \mathbf{r}_j} \quad \text{Polac-Ribière: } \beta_j = \frac{\mathbf{r}_{j+1}^T (\mathbf{r}_{j+1} - \mathbf{r}_j)}{\mathbf{r}_j^T \mathbf{r}_j} \\ &\text{Dai-Yuan: } \beta_j = \frac{\mathbf{r}_{j+1}^T \mathbf{r}_{j+1}}{\underline{\mathbf{p}}_j^T (\mathbf{r}_{j+1} - \mathbf{r}_j)} \quad \text{Hestenes-Stiefel: } \beta_j = \frac{\mathbf{r}_{j+1}^T (\mathbf{r}_{j+1} - \mathbf{r}_j)}{\underline{\mathbf{p}}_j^T (\mathbf{r}_{j+1} - \mathbf{r}_j)} \end{aligned} \tag{34}$$

  Moreover it is often chosen to avoid negative steps by using $\beta_j \leftarrow \max(0, \beta_j)$. The reader may refer to [17] and associated bibliography for more details. In our examples, the Polac-Ribière formula appeared to be more stable.

Algorithm 4: Non-invasive nonlinear conjugate gradient

Arbitrary initialization $\mathbf{p}_0$
$[\mathbf{u}_0^G] = \texttt{SolveGlobal}(\mathbf{p}_0; \mathbf{f}^G)$
$[\mathbf{u}_0^F, \boldsymbol{\lambda}_0^F] = \texttt{SolveFine}(\mathbf{u}_0^G; \mathbf{f}^F)$ // $[\boldsymbol{\lambda}_0^A] = \texttt{SolveAux}(\mathbf{u}_0^G; \mathbf{f}^A)$
Post-process: $\boldsymbol{\lambda}_0^C = \mathbf{p}_0 - \boldsymbol{\lambda}_0^A$, $\mathbf{r}_0 = -(\boldsymbol{\lambda}_0^F + \boldsymbol{\lambda}_0^C)$
Initialization: $\underline{\mathbf{p}}_0 = \mathbf{r}_0$
for $j \in [0, \cdots, m]$ **do**
  for *samples* $(\alpha_{j,i})_i$ **do**
    Preconditioning: $[\mathbf{u}_{j,i}^G, \boldsymbol{\lambda}_{j,i}^C] = \texttt{SolveGlobal}(\mathbf{p}_j + \alpha_{j,i} \underline{\mathbf{p}}_j; \mathbf{f}^G)$
    $[\mathbf{u}_{j,i}^F, \boldsymbol{\lambda}_{j,i}^F] = \texttt{SolveFine}(\mathbf{u}_{j,i}^G; \mathbf{f}^F)$ // $[\boldsymbol{\lambda}_{j,i}^A] = \texttt{SolveAux}(\mathbf{u}_{j,i}^G; \mathbf{f}^A)$
    Post-process: $\boldsymbol{\lambda}_{j,i}^C = \mathbf{p}_{j,i} - \boldsymbol{\lambda}_{j,i}^A$, $\mathbf{r}_{j,i} = -(\boldsymbol{\lambda}_{j,i}^F + \boldsymbol{\lambda}_{j,i}^C)$
  end
  Optimal step size (Line search): choose $I = \arg\min_i \|\mathbf{r}_{i,j}\|$
  Updates: $\mathbf{p}_{j+1} = \mathbf{p}_j + \alpha_{j,I} \underline{\mathbf{p}}_j$; $\mathbf{u}_{j+1}^{F,G} \leftarrow \mathbf{u}_{j,I}^{F,G}$; $\mathbf{r}_{j+1} \leftarrow \mathbf{r}_{j,I}$
  Pseudo-orthogonalization: $\underline{\mathbf{p}}_{j+1} = \mathbf{r}_{j+1} - \beta_j \underline{\mathbf{p}}_j$ with β_j given by formula (34)
end

4.5 Numerical illustration

The method is first illustrated on an academic 2D test case modeling a high pressure turbine blade of a plane engine (see figure 1). The Reference model possesses local perforations with adapted mesh which are not present in the Global model. Note that in that case, the Fine model is naturally more flexible than the Auxiliary model (because of the holes and the refined mesh). The Fine model is granted an elastoviscoplastic behavior of the form of [32] modeling a realistic IN100 material at hot temperature ($\simeq 1\,500°C$). We consider two configurations: in the first case the Complement model is linear (and so is the Global model), in the second case all models are elastoviscoplastic.

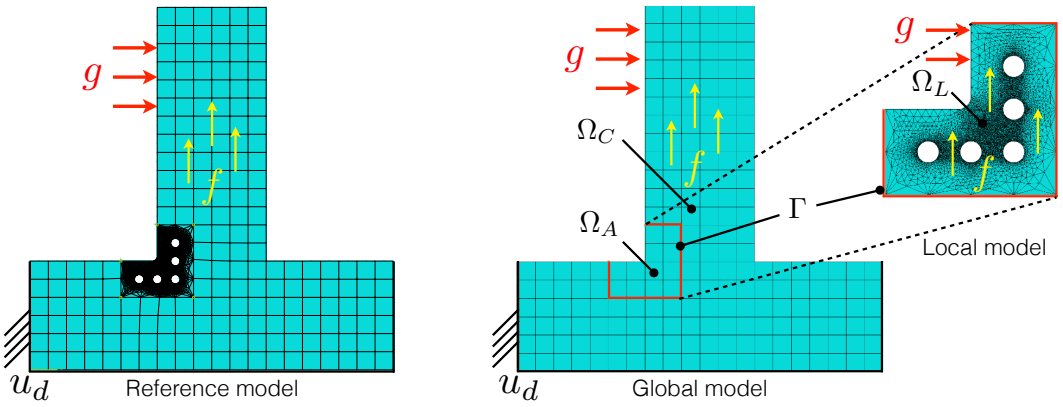

Figure 1: 2D test case

4.5.1 Linear Global model

We study the various acceleration strategies presented above in the case where the Complement zone is linear and the Auxiliary model is chosen to be so. Figure 2a presents the evolution of the Euclidean norm of the residual on the interface. As expected conjugate gradient is faster than other acceleration techniques. Figure 2b presents the evolution of the error measured by the Mises stress on the most loaded element with respect to the Reference model (which should not be available in production cases). We observe an important practical difficulty: Abaqus' truncation of Gauss point data makes it impossible to observe convergence beyond a relative precision of 10^{-6}. This problem would appear much later on the residual which only involves nodal computations (which can be manipulated in double precision).

Table 1 compares the duration of the computation. In that simple case all accelerations have close performance, but we observe that CG is faster than Aitken which is faster than SR1 which is 25% faster than Stationary iteration.

Method	Stat.	SR1	Aitken	CG
CPU time	2'55	2'11	1'57	1'47

Table 1: CPU time for various methods in the case of a linear Global model

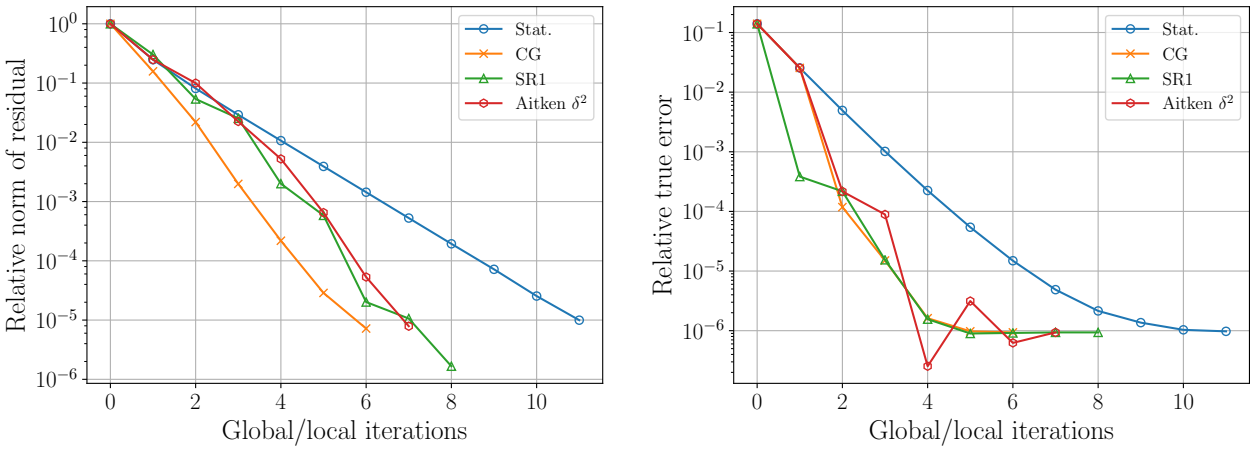

(a) Evolution of the residual

(b) Mises stress error wrt Reference on the most loaded element

Figure 2: Convergence of 2D case with linear Global model

4.5.2 Nonlinear Complement model

In that case, all models are granted the same nonlinear elastoviscoplastic behavior. As a consequence, plasticity may spread in the Complement zone. In that case the Fine and Auxiliary models only differ by their topology and their mesh.

Before comparing the acceleration techniques, we specifically study the choice of the parameters of the nonlinear conjugate gradient. Prior experiments showed that, for problems close to the one considered here, the optimal line-search always often belongs to the interval $[.8, 1.4]$, we thus use either 4 sampling points $\{.8, 1., 1.2, 1.4\}$ or 9 sampling points $\{.8, 1., 1.1, 1.15, 1.2, 1.25, 1.3, 1.35, 1.4\}$ where the sampling will be performed.

Figure 3 presents the performance of conjugate gradient for various conjugation techniques and various samplings for the linesearch. We observe that, in that case, the Polac-Ribière conjugation gives best results, and testing 9 lengths seems to be significantly superior to only testing 4. We recall that the line search is conducted in parallel so that oversampling does not take more wallclock time, it only "wastes" machine time and software licenses.

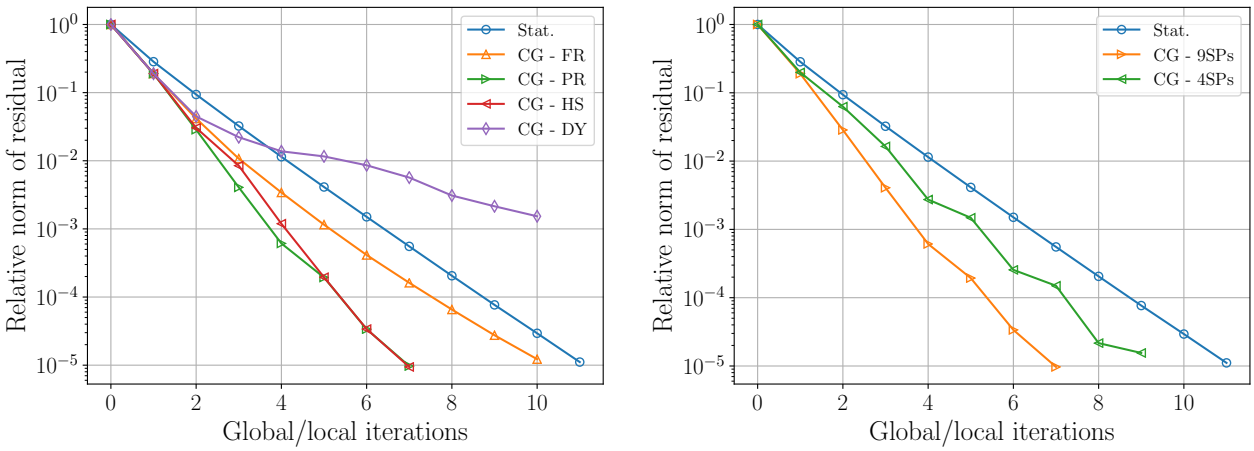

(a) Performance of "conjugation" formulae

(b) Influence of the linesearch sampling

Figure 3: Study of variants of nonlinear conjugate gradient

We compare, in Figure 4, the better configuration of conjugate gradient to other acceleration techniques. We observe that nonlinear conjugate gradient also behave better than the other techniques. Note that since the sampling of linesearch can be conducted in parallel, so that in practice one iteration of CG is faster than the one of the very cheap Aitken's method.

5 Overlapping version

In previous sections, we had assumed that the interface was described as the boundary of elements for all models. In practice this hypothesis is not so restrictive because most often the zone of interest is detected after an initial computation on the coarse global model, and it is constituted as a set of coarse elements satisfying a certain criterion. Even after remeshing, the boundary of the Fine description of the zone of interest matches a set of coarse faces (edges in 2D). Then a "simple" transfer matrix $\mathbf{T}$ can be sufficient to communicate between models on the interface. In particular, the easy choice of $\mathbf{T}$ being the interpolation matrix of the coarse kinematics in the fine kinematics can be implemented in most software. More evolved choices like mortar connections can also be employed in certain software.

We propose here an alternative strategy which makes use of the possibility to have the models overlap. In that case, there is no restriction on the definition of the meshes. This idea can directly be connected to overlapping optimized Schwarz methods, yet we propose a mechanical interpretation of it.

Note that the use of the overlap can be advantageous in the situations where edge effects can affect the fine model, even if meshes are conforming at the interfaces [19].

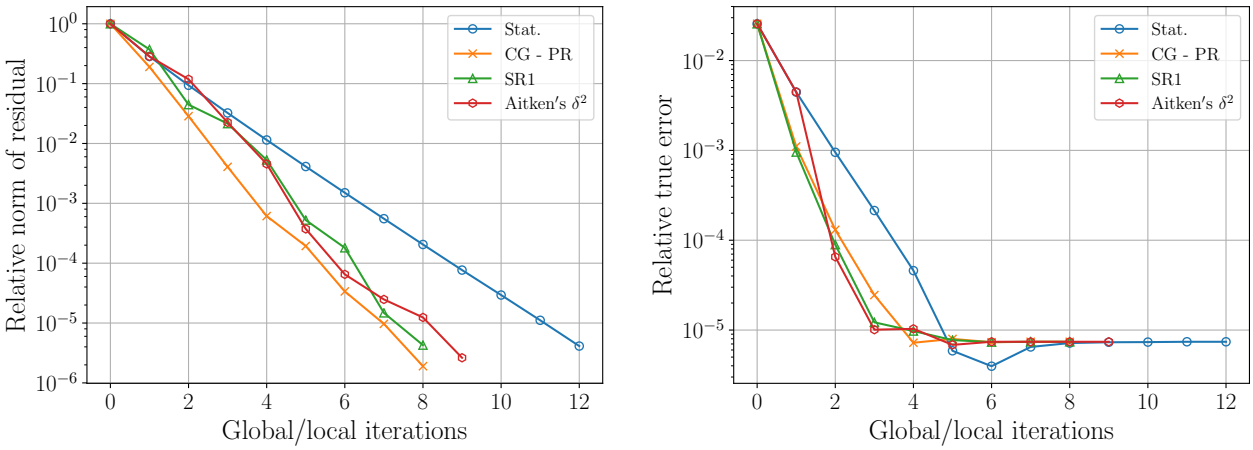

(a) Evolution of the residual

(b) Mises stress error wrt Reference on the most loaded element

Figure 4: Convergence of 2D nonlinear case

5.1 Handling of incompatible patches

The starting point is the observation that the method can be formulated as the search for $\mathbf{p}$ which is the stress discontinuity on the Global model between the Complement zone and the Auxiliary description of the zone of interest. This discontinuity must be such that the Complement zone is in equilibrium with the Fine description of zone of interest loaded with Dirichlet conditions (29).

Since $\mathbf{p}$ is a discontinuity, in order it to be well described in the coarse finite element model, it must be supported by the boundary of coarse elements. But there is no need for the support of $\mathbf{p}$ to match the boundary of the zone of interest.

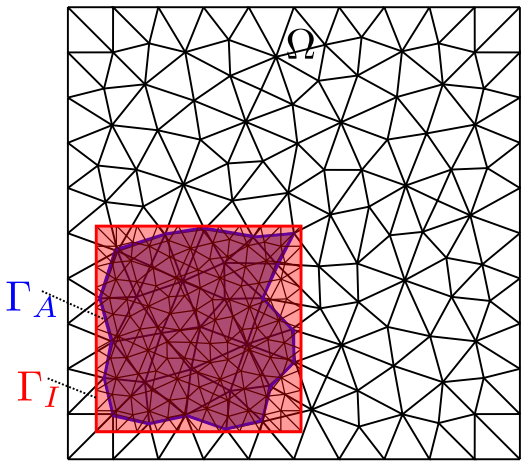

Figure 5: Technique with overlap for non-conforming meshes

We thus propose to follow the figure 5. The Fine subdomain Ω^F is positioned where needed in the zone of interest, its mesh is independent from the coarse mesh. We note $\Gamma^F = \partial\Omega^F$ the boundary of the Fine subdomain. The Auxiliary subdomain is the largest set of coarse elements fully contained in the zone of interest. We note Γ^A the boundary of the Auxiliary zone. The two interfaces Γ^F and Γ^A thus do not coincide. Ω^C is defined as the Complement to Ω^A in the Global problem.

Algorithm 5 gives the basic stationary iteration in the presence of overlap, all accelerations can be considered. In order to distinguish between the interfaces, the Auxiliary and the Fine problems are written on separate lines even if they can be solved in parallel.

The main difficulty of this algorithm is the computation of the Fine reaction on Γ^A with Ω^F not exactly represented on the coarse grid. This computation mixes the Fine stress σ_h^F and the coarse shape functions ϕ_i^G.

Algorithm 5: Non-invasive stationary iterations with overlap

Arbitrary initialization $\mathbf{p}_0$

for $j \in [0, \cdots, m]$ **do**

$[\mathbf{u}_j^G] = \texttt{SolveGlobal}(\mathbf{p}_j \text{ on } \Gamma^A; \mathbf{f}^G)$

$[\boldsymbol{\lambda}_j^A] = \texttt{SolveAux}(\mathbf{u}_j^G \text{ on } \Gamma^A; \mathbf{f}^A)$

$$\begin{cases} \mathbf{u}^F_{\Gamma^F,i} = u^G(x_i) \text{ for } i \text{ a Fine dof of } \Gamma^F \\ [\mathbf{u}_j^F, \sigma_{h,j}^F] = \texttt{SolveFine}(\mathbf{u}^F_{\Gamma^F,j}; \mathbf{f}^F) \end{cases}$$

$$\begin{cases} \text{for } i \text{ spanning all Global degrees of freedom on } \Gamma^A \\ \boldsymbol{\lambda}^F_{j,i} = \displaystyle\int_{\Omega^A} \left(\sigma^F_{h,j} : \varepsilon(\phi_i^G) - f \cdot \phi_i^G\right) dx - \int_{\partial_n \Omega^A} g \cdot \phi_i^G dS \end{cases}$$

Residual: $\mathbf{r}_j = -(\boldsymbol{\lambda}_j^F + \mathbf{p}_j - \boldsymbol{\lambda}_j^A)$

Update: $\mathbf{p}_{j+1} = \mathbf{p}_j + \mathbf{r}_j$;

end

Even if complex, this computation is feasible in certain software. Anyhow in the nonlinear case, σ_h^F is only known at Fine Gauss points and the integral can only be approximated.

There is another conceptual difficulty which is common to many methods with overlap [2]: the definition of a monolithic reference problem. Indeed the domain between the interfaces (the overlap) is a buffer zone Ω^B ($\Gamma^A \cup \Gamma^F = \partial\Omega^B$) where the Complement and the Fine model coexist. At convergence they are equivalent in the sense that they have the same value (up to transfer error) on Γ^F (Dirichlet) and Γ^A (Neumann) and they solve the same problem in the overlap.

5.2 Illustration of the coupling with overlap

The overlap was used in [19] for the coupling between a Global laminate plate model and a Fine 3D model. Various plate-to-3D transfer techniques were tried but it appeared that 3D edge effects were impossible to avoid completely. Figure 6 shows the variation of the peeling stress in the Fine 3D model direction orthogonal to the interface for various lifting of the plate displacement (named "Lagrangian" and "warping" in the figure). We see that edge effects are important on the boundary of the Fine domain (Γ^F) but they fade quickly so that the boundary of the Auxiliary domain (Γ^A) can be positioned not too far inside the zone of interest. The domain between Γ^F and Γ^A was called the buffer zone and a width of two times the thickness was sufficient.

Note that the overlap also allows to apply any type boundary conditions on the Fine domain. For instance if the zone of interest bears Dirichlet conditions, it is possible to use Neumann boundary conditions on Γ^F.

As said earlier, in the case of non-matching meshes, the difficulty for the coupling with overlap is the computation of the fine reaction on Γ^A written $\boldsymbol{\lambda}^F_{j,i}$ in Algorithm 5. In [18], in the more complex case of plate/3D coupling, it was proposed to extract a band of Auxiliary elements connected to Γ^A and project on it the Fine stress (defined at the Gauss point of the Fine mesh). This was implemented in Code_Aster using existing routines (PROJ_CHAMP() with keyword ECLA_PG).

Figure 7 presents a simple application of an isotropic plate in flexion where the Global model is a solid plate with unstructured mesh with triangular elements and the 3D Fine model bears a hole and is meshed with structured hexahedral elements. At convergence, the continuity is ensured on Γ^F as well as the equilibrium on Γ^A.

6 Conclusion

The global/local non-invasive coupling technique is a convenient way to enrich a global coarse model, handled by a commercial software, with local features, handled by most the adapted software. In this paper we proposed to interpret the method as an alternate non-overlapping Schwarz domain decomposition method. In this framework the coarse representation of the zone of interest is a clever way to build an approximation of the Dirichlet-to-Neumann operator of the Fine model, which includes the effects of the imposed load. Belonging to the Schwarz family of domain decomposition method allows to benefit many theoretical results and practical shrewdness.

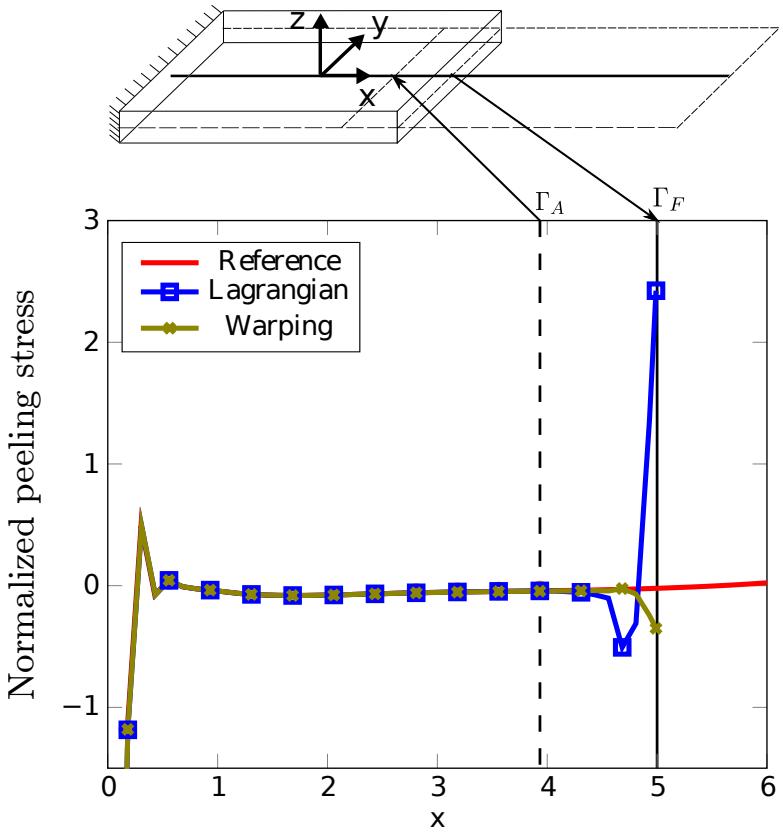

Figure 6: Plate/3D coupling: use of the overlap to avoid edge effects.

We then derive a conjugate gradient solver in the linear and nonlinear cases, in that later case the line search is realized by a sampling which can be conducted in parallel in order not to penalize the wallclock time. Finally we show that an overlapping version can also be applied which enables to connect non-matching meshes.

Acknowledgement: this work was partially funded by the French National Research Agency as part of project ICARE (ANR-12-MONU-0002-04). The authors wish to thanks Guillaume Guguin for the figures related to the non-conforming overlaping meshes.

References

[1] L. Badea. On the Schwarz alternating method with more than two subdomains for nonlinear monotone problems. *SIAM Journal on Numerical Analysis*, 28(1):179–204, 1991.

[2] H. Ben Dhia. Multiscale mechanical problems: the Arlequin method. *Comptes Rendus de l'Academie des Sciences Series IIB Mechanics Physics Astronomy*, 326(12):899–904, 1998.

[3] Omar Bettinotti, Olivier Allix, and Benoît Malherbe. A coupling strategy for adaptive local refinement in space and time with a fixed global model in explicit dynamics. *Computational Mechanics*, pages 1–14, 2013.

[4] Omar Bettinotti, Olivier Allix, Umberto Perego, Victor Oncea, and Benoît Malherbe. A fast weakly intrusive multiscale method in explicit dynamics. *International Journal for Numerical Methods in Engineering*, 100(8):577–595, 2014.

[5] Omar Bettinotti, Olivier Allix, Umberto Perego, Victor Oncea, and Benoît Malherbe. Simulation of delamination under impact using a global local method in explicit dynamics. *Finite Elements in Analysis and Design*, 125:1–13, 2017.

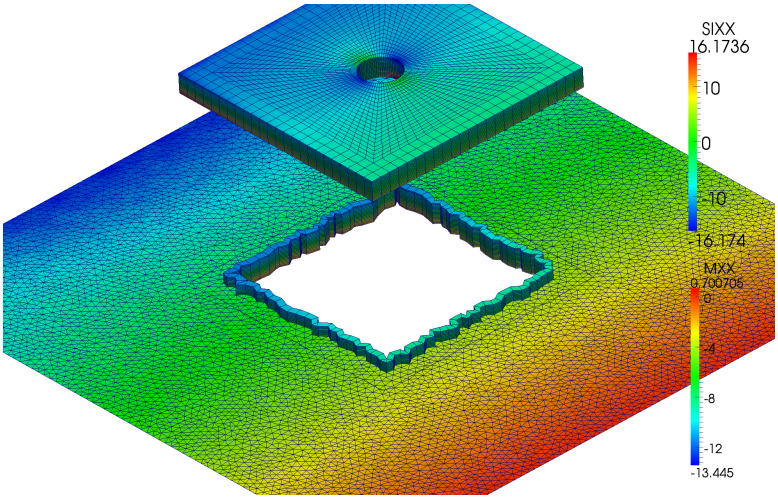

Figure 7: Exploded view of the plate/3D coupling with non-matching meshes. The interior of the Auxiliary model is not drawn in order to better see the intermediate mesh used for the stress projection.

[6] M. Chevreuil, A. Nouy, and E. Safatly. A multiscale method with patch for the solution of stochastic partial differential equations with localized uncertainties. *Computer Methods in Applied Mechanics and Engineering*, 255(0):255 – 274, 2013.

[7] P.G. Ciarlet. *Linear and nonlinear functional analysis with applications*. SIAM, Philadelphia, 2013.

[8] N. G. Cormier, B. S. Smallwood, G. B. Sinclair, and G. Meda. Aggressive submodelling of stress concentrations. *International Journal for Numerical Methods in Engineering*, 46(6):889–909, 1999.

[9] Philippe Cresta, Olivier Allix, Christian Rey, and Stéphane Guinard. Nonlinear localization strategies for domain decomposition methods: application to post-buckling analyses. *Computer Methods in Applied Mechanics and Engineering*, 196(8):1436–1446, 2007.

[10] M. Duval, J.-C. Passieux, M. Salaün, and S. Guinard. Local/global non-intrusive parallel coupling for large scale mechanical analysis. In *11th World Congress on Computational Mechanics - 5th European Conference on Computational Mechanics. IACM-ECCOMAS*, 2014.

[11] Mickaël Duval, Jean-Charles Passieux, Michel Salaün, and Stéphane Guinard. Non-intrusive coupling: recent advances and scalable nonlinear domain decomposition. *Archives of Computational Methods in Engineering*, pages 1–22, 2014.

[12] M. Feistauer and A. Zenisek. Finite element solution of nonlinear elliptic problems. *Numerische Mathematik*, 50:451–475, 1987.

[13] M. Gander, F. Magoulès, and F. Nataf. Optimized Schwarz methods without overlap for the Helmoltz equation. *SIAM J. Sci. Comput.*, 24(1):38–60, 2002.

[14] Martin J. Gander and Laurence Halpern. *Mathématiques pour l'ingénieur*, chapter Méthodes de décomposition de domaines. Techniques de l'Ingénieur, Saint-Denis, France, 2012.

[15] L Gendre, O Allix, and P Gosselet. A two-scale approximation of the Schur complement and its use for non-intrusive coupling. *International Journal for Numerical Methods in Engineering*, 87(9):889–905, 2011.

[16] Lionel Gendre, Olivier Allix, Pierre Gosselet, and François Comte. Non-intrusive and exact global/local techniques for structural problems with local plasticity. *Computational Mechanics*, 44(2):233–245, 2009.

[17] R. Glowinski. *Variational Methods for the Numerical Solution of Nonlinear Elliptic Problems*. Society for Industrial and Applied Mathematics, Philadelphia, PA, 2015.

[18] Guillaume Guguin. *Stratégie non-intrusive de couplage plaque/3D pour l'application aux plaques composites stratifiées*. PhD thesis, École Normale Supérieure de Cachan, Nov. 2014.

[19] Guillaume Guguin, Olivier Allix, Pierre Gosselet, and Stéphane Guinard. Nonintrusive coupling of 3d and 2d laminated composite models based on finite element 3d recovery. *International Journal for Numerical Methods in Engineering*, 98(5):324–343, 2014.

[20] Guillaume Guguin, Olivier Allix, Pierre Gosselet, and Stéphane Guinard. On the computation of plate assemblies using realistic 3d joint model: a non-intrusive approach. *Advanced Modeling and Simulation in Engineering Sciences*, 3(16), 2016.

[21] D. Hauer. The p-Dirichlet-to-Neumann operator with applications to elliptic and parabolic problems. *Journal of diffential equations*, 259(8):3615–3655, 2015.

[22] F. Hecht, A. Lozinski, and O. Pironneau. Numerical zoom and the Schwarz algorithm. In *Proceedings of the 18th conference on domain decomposition methods*, 2009.

[23] J. Hinojosa, O. Allix, P.A. Guidault, and P. Cresta. Domain decomposition methods with nonlinear localization for the buckling and post-buckling analyses of large structures. *Advances in Engineering Software*, 70:13–24, 2014.

[24] C. C. Jara-Almonte and C. E. Knight. The specified boundary stiffness/force SBSF method for finite element subregion analysis. *International Journal for Numerical Methods in Engineering*, 26(7):1567–1578, 1988.

[25] FS Kelley. Mesh requirements for the analysis of a stress concentration by the specified boundary displacement method. In *Proceedings of the Second International Computers in Engineering Conference, ASME*, pages 39–42, 1982.

[26] David E Keyes. Aerodynamic applications of Newton-Krylov-Schwarz solvers. In *Fourteenth International Conference on Numerical Methods in Fluid Dynamics*, pages 1–20. Springer, 1995.

[27] J. Kim and C.A. Duarte. A new generalized finite element method for two-scale simulations of propagating cohesive fractures in 3-d. *International Journal for Numerical Methods in Engineering*, 103(13):1139–1172, 2015.

[28] P. Ladevèze. Sur une famille d'algorithmes en mécanique des structures. *Comptes Rendus Académie des Sciences - Mécanique, Paris*, 300(2):41–45, 1985.

[29] P. Ladevèze. *Nonlinear Computational Structural Mechanics – New Approaches and Non-Incremental Methods of Calculation*. Springer Verlag, Berlin, 1999.

[30] Pierre Ladevèze. *Nonlinear computational structural mechanics: new approaches and non-incremental methods of calculation*. Springer, Berlin, 1999. translation by J. Simmonds.

[31] Y.J. Liu, Q. Sun, and X.L. Fan. A non-intrusive global/local algorithm with non-matching interface: Derivation and numerical validation. *Computer Methods in Applied Mechanics and Engineering*, 277:81–103, 2014.

[32] A. Longuet, A. Burteau, F. Comte, and A. Crouchez-Pilot. Incremental lifing method applied to high temperature aeronautical component. *CSMA 2013*, 2013.

[33] Camille Negrello, Pierre Gosselet, Christian Rey, and Julien Pebrel. Substructured formulations of nonlinear structure problems — influence of the interface condition. *International Journal for Numerical Methods in Engineering*, 107(13):1083–1105, 2016.

[34] Anthony Nouy and Florent Pled. A multiscale method for semi-linear elliptic equations with localized uncertainties and non-linearities. *arXiv:1704.05331v2*, 2017.

[35] Jean-Charles Passieux, Julien Réthoré, Anthony Gravouil, and Marie-Christine Baietto. Local/global non-intrusive crack propagation simulation using a multigrid X-FEM solver. *Computational Mechanics*, pages 1–13, 2013.

[36] Julien Pebrel, Pierre Gosselet, and Christian Rey. Une approche par patchs pour les non linéarités localisées en calcul de structures. *18ème Congrès Français de Mécanique (Grenoble 2007)*, 2007.

[37] J. Plews, CA Duarte, and T. Eason. An improved non-intrusive global-local approach for sharp thermal gradients in a standard FEA platform. *International Journal for Numerical Methods in Engineering*, 91(4):426–449, 2011.

[38] Jonathan B Ransom, Susan L McCleary, Mohammad A Aminpour, and Norman F Knight Jr. Computational methods for global/local analysis. *NASA STI/Recon Technical Report N*, 92:33104, 1992.

[39] Ernest K. Ryu and Stephen Boyd. Primer on monotone operator methods. *Appl. Comput. Math.*, 15(1):3–43, 2016.

[40] R.E. Showalter. *Hilbert space methods for partial differential equations.* Monographs and studies in mathematics. Pitman, London (UK), 1977.

[41] R.E. Showalter. *Monotone operators in Banach space and nonlinear partial differential equations*, volume 49 of *Mathematical surveys and monographs.* American mathematical society, Providence (US), 1997.

[42] J. D. Whitcomb. Iterative global/local finite element analysis. *Computers and structures*, 40(4):1027–1031, 1991.

[43] J. D. Whitcomb and K. Woo. Application of iterative global/local finite-element analysis. part 1: linear analysis. *Communications in Numerical Methods in Engineering*, 9:745–745, 1993.